

EUROPHYSICS LETTERS

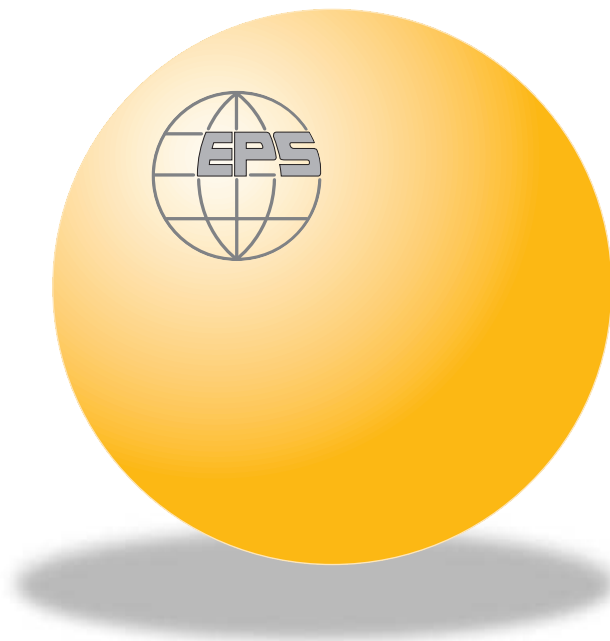
OFFPRINT

Vol. 68 • Number 3 • pp. 419–425

Wetting transitions on rough surfaces

* * *

C. ISHINO, K. OKUMURA and D. QUÉRÉ



Published under the scientific responsibility of the
EUROPEAN PHYSICAL SOCIETY
Incorporating
JOURNAL DE PHYSIQUE LETTRES • LETTERE AL NUOVO CIMENTO

Wetting transitions on rough surfaces

C. ISHINO¹, K. OKUMURA^{1(*)} and D. QUÉRÉ²

¹ *Department of Physics, Graduate School of Humanities and Sciences
Ochanomizu University - 2-1-1, Otsuka, Bunkyo-ku, Tokyo 112-8610, Japan*

² *Physique de la Matière Condensée, Collège de France, UMR 7125 du CNRS
11 place Marcelin-Berthelot, 75231 Paris Cedex 05, France*

received 24 March 2004; accepted in final form 1 September 2004

published online 9 October 2004

PACS. 68.08.Bc – Wetting.

PACS. 68.35.Md – Surface thermodynamics, surface energies.

PACS. 81.16.Nd – Nanolithography.

Abstract. – We consider microscopic contact states of a drop deposited on textured rough surfaces. The energies of three possible (meta)stable wetting states are compared and the lowest energy state is regarded as the “phase”. We present the “phase diagrams” in the two-dimensional space of texture parameters, which suggests transitions between the wetting states. We propose a model which allows the description of transition states between (meta)stable contact states and quantify the energy barriers between them. Thereby, we theoretically suggest that the actually realized state is not always the lowest energy state.

Introduction. – Recent technological advances allow us to design micro-scale structures on solid surfaces, and, consequently, to control the wettability of these solids, as shown both experimentally [1–8] and theoretically [9–13]. We discuss here the case of physically ragged surfaces rather than chemically inhomogeneous ones. It has been proposed that there can be at least three regimes for the contact area of drops on such jagged surfaces (fig. 1) [14]: (a) a Wenzel regime [15] where the solid/liquid interface exactly follows the solid roughness; (b) an air-pocket (AP) or Cassie regime, where air patches are confined below the drop, and (c) a penetration regime where an area surrounding the drop is impregnated by a liquid film.

We consider a small drop (to ignore the gravity) with a volume $V = 4\pi R_0^3/3$ (fig. 2a). Denoting γ as the liquid surface tension, the total surface energy of this drop is $E_0 = 4\pi R_0^2\gamma$. When it is deposited on a *flat* substrate, the contact angle θ is given by the relation of Young-Dupré:

$$\cos\theta = (\gamma_S - \gamma_{SL})/\gamma, \quad (1)$$

where γ_S and γ_{SL} are the surface tensions of the solid and the solid-liquid interface, respectively. The drop is a spherical cap of constant Laplace pressure whose radius is R (fig. 2b). Its total surface energy is given by $E_{\text{YD}} = \gamma S_C(\theta, R) + (\gamma_{SL} - \gamma_S)S_B(\theta, R)$, where

(*) E-mail: okumura@phys.ocha.ac.jp

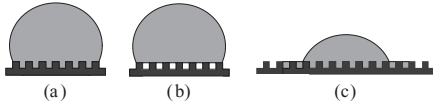


Fig. 1

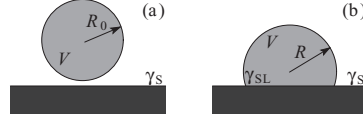


Fig. 2

Fig. 1 – Simplified illustration of three regimes: (a) Wenzel, (b) air pocket, and (c) penetration regimes.

Fig. 2 – (a) Reference state, (b) Laplace's spherical cap.

$S_C(\theta, R) = 2\pi R^2(1 - \cos\theta)$ and $S_B(\theta, R) = \pi R^2 \sin^2\theta$ are the areas of the liquid-gas and solid-liquid interfaces. The radius R is determined by the fixed volume condition:

$$V = \pi R^3 (1 - \cos\theta)^2 (2 + \cos\theta) / 3. \quad (2)$$

This gives a relation between R and R_0 [10], leading to the dimensionless energy of the Young-Dupré drop, $\varepsilon_{YD} \equiv E_{YD}/E_0$:

$$\varepsilon_{YD} = \varepsilon(\theta) \equiv 2^{-2/3} \left((1 - \cos\theta)^2 (2 + \cos\theta) \right)^{1/3}, \quad (3)$$

which is a monotonously increasing function of θ .

In this paper, we first derive such reduced energies for the three states sketched in fig. 1, and compare them with each other. Then, we demonstrate the possibility of observing and maintaining a state of higher energy, thanks to an energy barrier separating this state from another of smaller energy.

Three wetting states: Wenzel, air-pocket and penetration regimes. – In the Wenzel regime, the apparent contact angle θ_W is given as a function of r and θ :

$$\cos\theta_W = r \cos\theta, \quad (4)$$

where r is the *roughness factor*, *i.e.*, the ratio of the actual area wet by the liquid to its projection; r is larger than unity if the surface is not a perfect plane. The radius R_W of the cap is determined by eq. (2) by replacing (R, θ) with (R_W, θ_W) , provided that the scale of the texture is much smaller than the drop size. The total surface energy of the Wenzel state is simply given by $E_W = \gamma S_C(\theta_W, R_W) + (\gamma_{SL} - \gamma_S)r S_B(\theta_W, R_W)$ and the reduced energy $\varepsilon_W = E_W/E_0$ can be expressed as a function of θ and r via $\theta_W(\theta, r)$:

$$\varepsilon_W(\theta, r) = \varepsilon(\theta_W) \quad (5)$$

with the definition of $\varepsilon(\theta)$ in eq. (3). Equation (4) suggests a threshold value $r_m = 1/|\cos\theta|$ for r , above which the contact angle is π (hydrophobic case, *i.e.*, $\theta > \pi/2$) or 0 (hydrophilic case). Accordingly, we set $\varepsilon_W(\theta, r) = 1$ or 0 for $r > r_m$.

The Cassie-Baxter model describes the wettability of a chemical patchwork, composed of two materials of respective proportions f_1 and f_2 ($f_2 = 1 - f_1$) and of Young contact angles θ_1 and θ_2 [16]. The apparent contact angle θ^{**} on this patchwork is then given by

$$\cos\theta^{**} = f_1 \cos\theta_1 + f_2 \cos\theta_2. \quad (6)$$

The Cassie-Baxter model can be applied to the air-pocket regime (fig. 1b), the material being a composite of solid and air. Namely, we have $\theta_1 = \theta$ and $\theta_2 = \pi$ (the “contact angle” of

a drop on air). The fraction of the first component f_1 corresponds to the solid surface fraction ϕ_S wet by the liquid. Noting $f_1 + f_2 = 1$ in the original model, we find

$$\cos \theta_{AP} = \phi_S (\cos \theta + 1) - 1. \quad (7)$$

The radius R_{AP} of the cap is determined again by eq. (2), by replacing (R, θ) with (R_{AP}, θ_{AP}) . The total surface energy is now calculated as $E_{AP} = \gamma[S_C(\theta_{AP}, R_{AP}) + (1 - \phi_S)S_B(\theta_{AP}, R_{AP})] + (\gamma_{SL} - \gamma_S)\phi_S S_B(\theta_{AP}, R_{AP})$. Note here that a fraction ϕ_S of the bottom area is in contact with liquid ($\gamma_{SL} - \gamma_S$) while the remaining portion ($1 - \phi_S$) is exposed to the gas phase (γ). The normalized energy $\varepsilon_{AP} = E_{AP}/E_0$ is expressed as

$$\varepsilon_{AP}(\theta, \phi_S) = \varepsilon(\theta_{AP}). \quad (8)$$

The Cassie-Baxter model also describes the penetration regime (fig. 1c), for which the substrate is a composite of solid and liquid [17]. We have $\theta_1 = \theta$, $\theta_2 = 0$ (the ‘‘contact angle’’ of a liquid on itself), $f_1 = \phi_S$, and $f_2 = 1 - \phi_S$, which yields

$$\cos \theta_P = \phi_S (\cos \theta - 1) + 1. \quad (9)$$

To calculate the total surface energy associated with this situation, we introduce the area S_D of the penetration ‘‘film’’ developed around the drop, *where the cavities are filled with the liquid while the top of the texture remains dry* (see fig. 1c). With this doughnut-shaped S_D , the total surface energy can be written as $E_P = \gamma S_C(\theta_P, R_P) + (\gamma_{SL} - \gamma_S)r S_B(\theta_P, R_P) + [(r - \phi_S)(\gamma_{SL} - \gamma_S) + (1 - \phi_S)\gamma]S_D$.

How can we find S_D or $\Sigma \equiv S_D + S_B(\theta_P, R_P)$? First of all, Σ must be macroscopically larger than the (apparent) bottom area $S_B(\theta_P, R_P)$, since eq. (9) assumes the development of such a wet front (otherwise the angle should be given by eq. (4) or others). In addition, if the coefficient of Σ or S_D in the above expression for E_P is negative, *i.e.*,

$$C \equiv -(r - \phi_S) \cos \theta + 1 - \phi_S = \cos \theta_P - \cos \theta_W < 0, \quad (10)$$

the energy E_P is lowered as the film progresses [17]. Then, the doughnut expands as far as possible, and its only limitation is the solid size or the finite volume of the drop, from which we can set this to be the lowest energy state if $C < 0$; we need not to know the exact value of Σ . This special lowest energy state realized when $C < 0$ shall be called ‘‘large penetration (LP)’’. On the other hand, if $C > 0$, the drop reduces to a Wenzel drop with the penetration angle θ_P (small penetration, SP). To summarize, we find

$$E_P \sim \begin{cases} E_{LP} = \gamma \Sigma C & (C < 0), \\ E_{SP} = \gamma \pi R_P^2 [2(1 - \cos \theta_P) - r \cos \theta_P \sin^2 \theta_P] & (C > 0). \end{cases} \quad (11)$$

From eqs. (9) and (11) with the (approximate) formula for the radius R_P (*i.e.*, eq. (2) with $(R, \theta) \rightarrow (R_P, \theta_P)$), we obtain the dimensionless energy $\varepsilon_P(\theta, r, \phi_S)$.

We compare $\varepsilon_W(\theta, r)$, $\varepsilon_{AP}(\theta, \phi_S)$, and $\varepsilon_P(\theta, r, \phi_S)$ as a function of the parameters r and ϕ_S with θ and V fixed in order to determine the lowest energy state. The results are universal in the sense that they are independent of γ and V .

The results of the comparison are displayed in fig. 3 in the (r, ϕ_S) -plane, where the lowest energy regimes are indicated. For hydrophobic substrates ($\theta > \pi/2$) either the Wenzel or AP state has the lowest energy (fig. 3a). On the contrary, for hydrophilic substrates (fig. 3b), it is the AP regime that does not show up; the AP regime in the hydrophobic case is just replaced

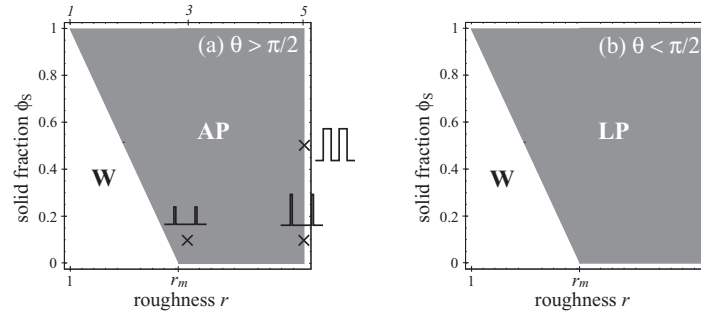


Fig. 3 – “Phase” diagrams of contact states (a) for a hydrophobic substrate and (b) for a hydrophilic substrate. W (Wenzel), AP, LP indicate the lowest energy state in the region. Examples of textures are indicated in the left picture for $\cos \theta = -0.35$ (upper horizontal italic scale r is for this θ).

by the LP regime. Figure 3 indicates the transition from the Wenzel to AP (LP) regime with increase in r and ϕ_S for the hydrophobic (hydrophilic) case.

We can confirm analytically that the boundary between the two regimes is given by $C = 0$ or $\cos \theta_P = \cos \theta_W$ in the hydrophilic case and by $\cos \theta_{AP} = \cos \theta_W$ in the hydrophobic case (we can understand this noting that $\varepsilon(\theta)$ is an increasing function of θ). From fig. 3, the AP state is the lowest energy if $\theta_{AP} < \theta_W$ in the hydrophobic case [11], while the LP state is the lowest if $\theta_P > \theta_W$ in the hydrophilic case (indeed, the latter condition or eq. (10) was originally derived as the condition of penetration of the “film” [17]).

Energy barriers. – Experimentally, AP state can be observed on a hydrophilic substrate (on hydrophilic substrates decorated with posts, advancing angles larger than 90° can be measured, indicating air trapping). In addition, an AP state can be changed into a Wenzel state (with fixed r and ϕ_S) through an external perturbation, say, by pushing the drop [5]. This seems to contradict the phase diagrams obtained above, and suggests that the trapping to a metastable state may occur [5,11]. Such states are possible provided that energy barriers exist [11], and we propose here an extended model (for hydrophobic substrates) in order to quantify this point.

Imagine a transition from AP to Wenzel state: a simple pathway may start from lowering of the bottom, liquid-air interface (fig. 4a) towards a state where a very thin air film (with an infinitely small thickness l_1) remains at the bottom of the groove. The thin film is, then, invaded by the liquid (fig. 4b) until the Wenzel state is obtained.

The area of the liquid-air contact, $1-f$, is a constant ($f = \phi_S$) in the lowering stage (fig. 4a), while the roughness factor of the liquid surface under the drop (both the liquid-solid and liquid-air interfaces are counted), r' , is fixed to $r' = r$ in the invasion stage since l_1 is virtually zero (fig. 4b).

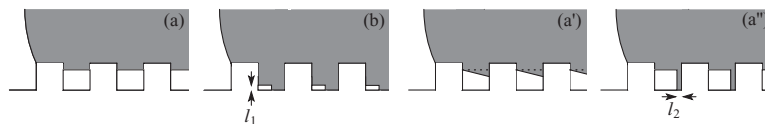


Fig. 4 – Transition states: (a) lowering stage ($f = \phi_S$ and $r' > 1$) and (b) invasion stage ($f > \phi_S$ and $r' = r$). States (a') and (a'') have larger energies than (a). Here, l_1 and l_2 are infinitely small.

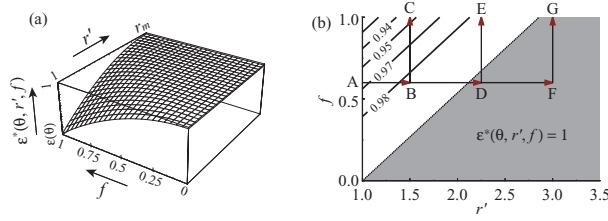


Fig. 5 – (a) Energy landscape $\varepsilon^*(\theta, r', f)$ for the extended model. This plot is independent of θ except for $r_m = 1/|\cos \theta|$. (b) The specific case with $\cos \theta = -0.35$ ($\theta \sim 110^\circ$) is shown as a contour plot, where r_m is specified to 2.9.

To incorporate these parameters r' and f into the Cassie-Baxter model, we regard f_1 (f_2) as the ratio of the liquid-solid (liquid-air) interface under the drop to the (apparent) bottom area of the drop (*i.e.*, $f_2 = 1 - f$ and $f_1 = r' - f_2$). With this identification, since $r' > 1$, $f_1 + f_2$ is allowed to deviate from one! In this extended Cassie-Baxter model for a composite of solid ($\theta_1 = \theta$) and air ($\theta_2 = \pi$), the contact angle θ^* is given by $\cos \theta^* = -f_2 + f_1 \cos \theta$:

$$\cos \theta^* = f - 1 + (r' + f - 1) \cos \theta, \quad (12)$$

where we set $\theta^* = \pi$ if the r.h.s. is smaller than -1 . Equation (12) can be derived as a stationary condition of the energy variation for a virtual displacement of the contact line like the other contact angle formulae of Young, Wenzel, and Cassie.

Equation (12) reduces to the Wenzel angle when $(r', f) = (r, 1)$ and to the AP angle when $(r', f) = (1, \phi_S)$; eq. (12) unifies the two regimes. Moreover, as desired, the lowering stage (fig. 4a) is described by an increase in r' with f fixed to ϕ_S , and the invasion stage (fig. 4b) by an increase in f with r' fixed to r . In addition, even states as in fig. 4a'' and a'' and more general situations are included in the model, as we shall see below.

It is useful to consider the space (r', f) . For convenience, we use the reduced energy ε^* as a function of r' and f with θ fixed, which can be derived as before. With eq. (12) and the function ε in eq. (3), the result is given by

$$\varepsilon^*(\theta, r', f) = \varepsilon(\theta^*), \quad (13)$$

where we set $\varepsilon^*(\theta, r', f) = 1$ if $\cos \theta^*$ in eq. (12) is smaller than -1 . The energy landscape on the (r', f) -plane is displayed in figs. 5a and b. The function with a fixed angle θ has the maximum, 1, in the region $f - 1 + (r' + f - 1) \cos \theta < -1$, and the minimum, $\varepsilon(\theta)$, at $(r', f) = (1, 1)$ where, from eq. (3), $\varepsilon(\theta) \sim 1$ for hydrophobic angles.

The *rectangular path* $A \rightarrow B \rightarrow C$ in fig. 5b describes the simple transition pathway from the AP to Wenzel state on the specific substrate characterized by $(r, \phi_S) = (1.5, 0.6)$: the point A in fig. 5b at $(r', f) = (1, \phi_S = 0.6)$ corresponds to the AP state while C at $(r', f) = (r = 1.5, 1)$ to the Wenzel states; $A \rightarrow B$ and $B \rightarrow C$ correspond to transition states in figs. 4a and b, respectively. Likewise the rectangular pathways $A \rightarrow B \rightarrow D \rightarrow E$ and $A \rightarrow B \rightarrow D \rightarrow F \rightarrow G$ follows the simple transition (AP \rightarrow Wenzel) on the substrates specified by $(r, \phi_S) = (2.25, 0.6)$ and $(3, 0.6)$, respectively (see the inserted drawings of the surface textures in fig. 6).

Energy barrier curves along these paths in fig. 5b are shown in fig. 6. Generally, from the landscape in fig. 5, transitions $W \rightleftharpoons AP$ via the rectangular path always encounters a barrier for any (r, ϕ_S) except for $r > r_m$ (no barrier for $W \rightarrow AP$ when $r > r_m$ as in fig. 6c).

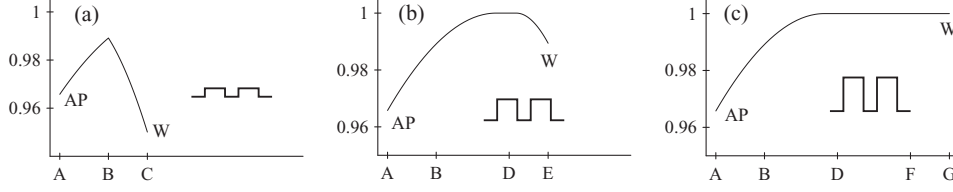


Fig. 6 – Energy barriers curve ε^* (a) for the texture with $r = 1.5$ and $\phi_S = 0.6$ (along the path $A \rightarrow B \rightarrow C$ in fig. 5), (b) for $r = 2.25$ and $\phi_S = 0.6$ ($A \rightarrow D \rightarrow E$) and (c) for $r = 3$ and $\phi_S = 0.6$ ($A \rightarrow F \rightarrow G$), where $\cos \theta = -0.35$. The surface textures are also shown with the plots.

The absolute value of the energy barrier can be huge, which seems consistent with experimental observations in [5]. The vertical axis in fig. 6 is scaled by $E_0 \sim \gamma R_0^2$; noting $\gamma \sim kT/a^2$ with a an atomic scale, an energy barrier of the order of E_0 is extremely large compared to the thermal fluctuation ($E_0/kT \sim (R_0/a)^2 \gg 1$).

What is the meaning of paths deviating from the rectangular path? Some paths are the ones with a higher barrier and the others are unphysical. The above rectangular path is the minimum-barrier path for the two-level texture design; for example, figs. 4a' and a'' are the cases with $f < \phi_S$ (not on the rectangular path) and have a larger energy than the state in fig. 4a (on the rectangular path) because $\gamma_{SL} - \gamma_S$ is always positive for hydrophobic substrates. For other texture design, say, triangular grooves, the minimum-barrier path becomes different from the above physical path (for triangular grooves, we may set $f_2 \rightarrow r_f f$ instead, where r_f is the roughness ratio of the wet area [12]).

An example of unphysical path in the present texture design is the barrier-free path directly connecting $(1, \phi_S)$ and $(r, 1)$ on the equal-energy line, that is, in parallel with the line $\cos \theta^* = -1$. Such a path may not be associated with a physically possible transition state on a fixed texture (specified by a single set of r and ϕ_S).

Conclusion and discussion. – We have explicitly compared the energy of the three wetting states (W, AP, and P) and obtained the phase diagram in the (r, ϕ_S) -plane, where the lowest energy state is identified with the phase, for both hydrophobic and hydrophilic substrates. We have proposed an extended model unifying the W and AP states to quantify the energy barriers between wetting states for the hydrophobic substrates. As a result, we have shown that a transition $W \rightarrow AP$ can be without a barrier when $r > r_m$; otherwise, W or AP is a metastable state where a barrier crossing is required to reach the lower (stable) energy state. This barrier is typically large compared to the thermal energy, which can be quantified in the unit of $E_0 = 4\pi\gamma R_0^2$ by compact formulae: the barriers for $W \rightarrow AP$ and $AP \rightarrow W$ transitions are respectively given by $\varepsilon(\theta_m) - \varepsilon(\theta_W)$ and $\varepsilon(\theta_m) - \varepsilon(\theta_{AP})$, with θ_W and θ_{AP} given by eqs. (4) and (7) and with θ_m being the value of θ^* in eq. (12) at $(r', f) = (r, \phi_S)$; note that the functions $\varepsilon(\theta)$ defined in eq. (3) should be set to 1 if the cosines of the corresponding angles $(\theta_m, \theta_W, \theta_{AP})$ are less than -1 . The details of calculations including a unified model for hydrophilic substrates and for various surface designs will be discussed elsewhere.

Comparison of our results with experiments requires a special care. For example, in [4], the wetting states on a hydrophobic substrate ($\theta = 114^\circ$) with textures of $\phi_S = 0.11$ and $\phi_S = 0.36$ are experimentally checked by changing r from 1 to ~ 3 , where the $W \rightarrow AP$ transition occurs at $r \simeq 1.2$ for both values of ϕ_S . Here, $r_m \simeq 2.46$ in fig. 3a and the transition indicated from this figure occurs at $r \simeq 2.3$ and $r \simeq 1.9$, respectively. This apparent disagreement is reasonable if we remind that there is an energy barrier so that experiments do not necessarily lead to the observation of the the lowest energy state; when $r \lesssim 2$ barriers of the type of

fig. 6a exist and the barrier crossings become easier when r approaches 1. In other words, for $r \simeq 1.2$ – 2.3 (or 1.9), the observed AP states are metastable and the drop cannot go over the barrier toward the lowest energy (Wenzel) state. We encountered the same tendency when examining other experimental data from [6, 7].

The above example reveals the importance of an unambiguous experiment monitoring which is the observed state and whether the state is stable or metastable, to test our equilibrium phase diagrams. Measurement of the contact angle hysteresis (which can be dramatically different in the W and in the AP regimes) allows us to distinguish the states, and the control of the (potential) transition between the states might be done by a compression of the drop [5]. Conveniently, the value of the critical pressure above which a transition occurs provides a way to evaluate the energy barrier between two states. However, the achievement of this program is far beyond the scope of this letter.

* * *

We thank P.-G. DE GENNES for discussions and encouragements and J. BICO and M. CALLIES for discussions.

REFERENCES

- [1] ONDA T., SHIBUICHI S., SATOH N. and TSUJII K., *Langmuir*, **12** (1996) 2125.
- [2] NEINHUIS C. and BARTHLOTT W., *Ann. Bot.*, **79** (1997) 667.
- [3] BICO J., MARZOLIN C. and QUÉRÉ D., *Europhys. Lett.*, **47** (1999) 220.
- [4] YOSHIMITSU Z., NAKAJIMA A., WATANABE T. and HASHIMOTO K., *Langmuir*, **18** (2002) 5818.
- [5] LAFUMA A. and QUÉRÉ D., *Nature Mater.*, **2** (2003) 457.
- [6] HE B., PATANKAR N. A. and LEE J., *Langmuir*, **19** (2003) 4999.
- [7] ONER D. and MCCARTHY T. J., *Langmuir*, **16** (2000) 7777.
- [8] NARHE R. and BEYSENS D., *Phys. Rev. Lett.*, **93** (2004) 076103.
- [9] SWAIN P. S. and LIPOWSKY R., *Langmuir*, **14** (1998) 6772.
- [10] EXTRAND C. W., *Langmuir*, **18** (2002) 7991; **19** (2003) 646.
- [11] PATANKAR N. A., *Langmuir*, **19** (2003) 1249; after we had completed this work, N. A. Patankar kindly sent us a preprint where a discussion on energy barriers can be found. The reference of this paper is PATANKAR N. A., *Langmuir*, **20** (2004) 7097.
- [12] MARMUR A., *Langmuir*, **19** (2003) 8343.
- [13] DUPUIS A. and YEOMANS J. M., *Mesoscopic modeling of droplets on topologically patterned substrates*, cond-mat/0401150.
- [14] DE GENNES P.-G., BROCHARD-WYART F. and QUÉRÉ D., *Gouttes, Bulles, Perles et Ondes* (Belin, Paris) 2002.
- [15] WENZEL R. N., *Ind. Eng. Chem.*, **38** (1936) 988.
- [16] CASSIE A. B. D. and BAXTER S., *Trans. Faraday Soc.*, **40** (1944) 546.
- [17] BICO J., TORDEUX C. and QUÉRÉ D., *Europhys. Lett.*, **55** (2001) 214.